Cleaner Engineering and Technology 5 (2021) 100284

Contents lists available at ScienceDirect

Cleaner Engineering and Technology

journal homepage: www.sciencedirect.com/journal/cleaner-engineering-and-technology

Performance of reverse osmosis based desalination process using spiral wound membrane: Sensitivity study of operating parameters under variable seawater conditions

S.H. Aladwani [a], M.A. Al-Obaidi [b], I.M. Mujtaba [a,*]

[a] Department of Chemical Engineering, Faculty of Engineering and Informatics, The University of Bradford. Bradford, West Yorkshire, BD7 1DP, UK
[b] Middle Technical University, Technical Institute of Baquba, Baquba, Dayala, Iraq

ARTICLE INFO

Keywords:
Reverse osmosis desalination
Spiral wound membrane
Modelling
Variable seawater conditions
Sensitivity analysis

ABSTRACT

Reverse Osmosis (RO) process accounts for 80% of the world desalination capacity. Apparently, there is a rapid increase of deploying the RO process in seawater desalination due to its high efficiency in removing salts at a reduced energy consumption compared to thermal desalination technologies such as MSF and MED. Among different types of membranes, spiral would membranes is one of the most used. However, there is no in-depth study on the performance of spiral wound membranes in terms of salt rejection, water quality, water recovery and specific energy consumption subject to wide range of seawater salinity, temperature, feed flowrate and pressure using a high fidelity but a realistic process model which is therefore is the focus of this study. The membrane is subjected to conditions within the manufacturer's recommendations. The outcome of this research will certainly help the designers selecting optimum RO network configuration for a large-scale desalination process.

1. Introduction

Water is the most important source in human's life, whoever a critical question is raised: does the freshwater amount is enough for all humans. The answer is there are several regions on the world suffering water shortage. As the freshwater forms less than 3% of the world water resources where it can be found underground, the rest of world water comes from oceans seas and lakes which present highly saline water and constitute a ratio around 97% of the world water resources (Oki and Kanae, 2006). Considering that and increased demand of freshwater, the desalination processes have reflected a lifeline for humans around the world. Desalination is used to produce freshwater and existed for a much longer time since it entirely tackles the water scarcity situation.

Reverse Osmosis (RO) is known to be a process used to remove contaminants such as salt and other dissolved compounds that make the water undrinkable by utilising semipermeable membranes that separate the contaminants from water and allow it to be entirely clean (Wenten, 2016). Permeate water is acquired once the feed water is driven inside the feed channel, these tiny molecules of water are permeated via the membrane pores and present pure water whereas the impurities are drained and are known to be a part of the reject water. Due to the semipermeable state of membranes, salt ions are not allowed to pass through with the rest of the clean water. There is no doubt that the RO process relies on these membranes to acquire drinkable water. There are different types of membrane modules used in RO process such as tubular spiral-wound and hollow-fibre membranes leading to satisfactory process performance. However, the application of these modules is dependent on the composition of the feed water as well as functionality of the plant (Alsarayreh et al., 2020). In addition, RO is taking the place of MSF and MED due to low energy consumption compared to the thermal desalination technologies (Woo et al., 2019).

Due to RO functionality, the performance can be evaluated by looking at the process ability to desalinate the saline water and the energy consumption required which is summarised below:

- Permeate salinity (*Cp*): As it is the objective function of this process, *Cp* is one of the performance indicators. The RO process is built up to minimize this value.
- Water recovery (*WR%*) and solute rejection (*SR%*): These are the amount of water recovered and the salt or other minerals rejected by RO process, respectively. *WR%* and *SR%* used to evaluate the RO process where they directly signify the process efficiency.

* Corresponding author.
E-mail address: I.M.Mujtaba@bradford.ac.uk (I.M. Mujtaba).

https://doi.org/10.1016/j.clet.2021.100284
Received 7 January 2021; Received in revised form 30 September 2021; Accepted 30 September 2021
Available online 2 October 2021

Nomenclature

$A_{w(T)}$	[m/atm s] Water transport coefficient at inlet temperature (T)
C_b	[kg/m^3] Solute concentrations at the feed channel of the membrane
C_f	[kg/m^3] Solute concentration of feed seawater
C_W	[kg/m^3] Solute concentration at the membrane surface at the feed channel
C_p	[kg/m^3] Solute concentration at the permeate channel
C_r	[kg/m^3] Solute concentration disposed out the membrane (retentate stream)
D_b	[m^2/s] Coefficient of solute diffusion of feed seawater at the feed channel
d_h	[m] The hydraulic diameter
Js	[kg/m^2 s] Solute flux of through the membrane's pores
J_w	[m/s] Water flux through the membrane's pores
K	[m/s] Mass transfer coefficient at the feed channel
L	[m] Length of the membrane
P_f	[atm] Feed pressure
P_p	[atm] Pressure at the permeate channel
Q_f	[m^3/s] Feed flow rate at the feed channel of the membrane
Q_p	[m^3/s] Permeate flow rate at the permeate channel
Q_r	[m^3/s] Retentate flow rate
Re	[dimensionless] Reynolds number
WR	[dimensionless] Water recovery
SR	[dimensionless] Solute rejection
T	[°C] Feed temperature
W	[m] Width of the membrane
μ_b	[kg/m s] Bulk viscosity of feed seawater
ρ_b	[kg/m^3] Bulk density of feed seawater
π_b	[atm] Bulk osmotic pressure of feed seawater
π_p	[atm] Osmotic pressure in the permeate channel
K_{dc}	[dimensionless] Characteristic of feed spacer

- Specific energy consumption (*EC*): What distinguishes the RO technology is the lower specific energy consumption compared to other water desalination technologies, which is known to be the least energy-consuming in this field (Carter, 2015). The less the specific energy consumption, the lower the cost of production. Worth noting that most of the energy is consumed by the pumps.

Seasonal variation of seawater salinity and temperature is caused by local features of water masses such as coastal upwelling, local winds and currents, or rainfall-runoff (Donguy and Meyers, 1996). Therefore, it is crucial to recognise the performance variation of any industrial desalination system including RO process against the variation of seawater conditions. However, in the past it was not widely considered. For example, for tubular membrane, Villafafila and Mujtaba (2003) considered maximising profitability of RO process while optimising design and operating parameters using irreversible thermodynamic model. For hollow fibre membrane, See et al. (1999) and Lu et al. (2006) minimised the total annualised cost (TAC) while optimising cleaning and membrane replacement schedules for RO process over a time horizon but used very simple RO model. Lu et al. (2007) considered minimisation of total annualised cost (TAC) while optimising RO network again using a very simple process model for spiral wound membrane. Saif et al. (2008) considered minimisation of total annualised cost (TAC) while optimising RO network again using a short-cut RO process model for hollow-fibre membrane. However, all these studies were limited to single seawater salinity and temperature.

Du et al., 2012 considered minimisation of total annualised cost (TAC) while optimising RO network for a wide range of seawater salinity and a fixed temperature for spiral wound membrane but using a simplified process model. Li (2012) developed a constrained nonlinear optimisation framework based mathematical model to optimise the operation of brackish water RO desalination system in order to minimize the total specific energy consumption. The validated model based experimental data was considered the membrane area, water flow, pump pressure, and pressure drop along the membranes length and validated by plant data. A total reduction of 16% can be attained in specific energy consumption via optimising the operating variables with constraining a fixed value of permeate flow. Sassi and Mujtaba (2011) considered simulation of a spiral wound RO process but using two values of extremely low feed salinity (2500 ppm, 5000 ppm) and a single seawater temperature. Sassi and Mujtaba (2012) considered minimisation of total annualised cost (TAC) while optimising RO network for a wide range of seawater salinity and temperature but using hollow-fibre membranes and a detailed process model. Al-Obaidi et al. (2018) studied the performance of multistage spiral wound RO process but subject to brackish water and limited variation in salinity (not in the range of seawater salinity) and temperature. More recently, Ruiz-García et al. (2020) studied the influence of inlet parameters of brackish water including feed flow rate, feed pressure and inorganic compositions on the efficiency of two configurations of two stages RO system of 2:1 and 3:2 pressure vessels (each pressure vessel contains 6 brackish water spiral wound membranes). The results confirmed average specific energy consumption and water recovery of 0.76 kWh/m^3, and 33.47%, respectively. Furthermore, Ruiz-García and Nuez (2020) proposed a simple on-off control strategy for enhancing the operation of six spiral wound elements stuffed in a pressure vessel connected with one and two stages of different configurations. In this regard, the variation of brackish water quality was considered where a simulation was carried out to select the most appropriate conditions of the lowest power entering the RO system. It was revealed that 3:2 configuration is the most suitable for most of the operating range.

As can be seen for the published literature, the performance of a spiral wound membrane subjected to a wide range of salinity, temperature, feed flowrate and pressure has not been studied using a high-fidelity realistic RO process model, which can be used for designing RO configuration and optimisation. Therefore, this has been the focus of this study. Here, the sensitivity analysis of the RO process is carried out to explore the behaviour of several performance metrics (salt rejection, freshwater quality, water recovery, specific energy consumption) against the variation of inlet parameters including feed salinity, pressure, flow rate and temperature.

2. Spiral wound RO membrane process and mathematical modelling

The proposed RO process is given in Fig. 1. This contains a high-pressure pump to feed the seawater inside the membrane module to

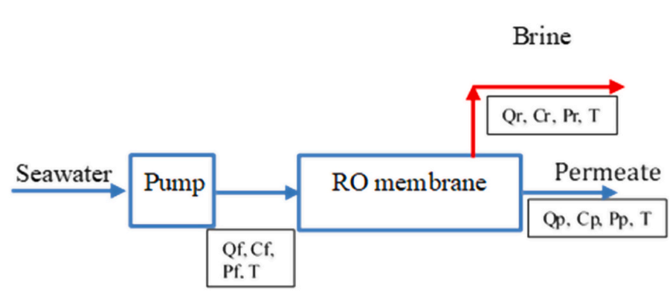

Fig. 1. Schematic diagram of RO desalination process.

remove the salts and produce two streams: one is high salinity brine stream, and the other is low salinity permeate stream.

Simulation of industrial processes has been widely used by several researchers to evaluate the performance and the levels of responses against the expected variations of operating conditions. Therefore, it is important to utilise a comprehensive model in a simulation-based study to critically evaluate the process efficiency before using the model for design and optimisation. The comprehensive model used in this work was already developed by the same authors (Al-Obaidi et al., 2018) as detailed below.

Total material and mass balance are

$$Q_f = Q_r + Q_p \tag{1}$$

$$Q_f C_f - Q_r C_r = Q_p C_p \tag{2}$$

Water flux is quite related to net driving pressure and water transport parameter of the membrane as presented in Eq. 3

$$Jw = NDP\ Aw(T) \tag{3}$$

$$NDP = P_b - P_p - \pi_b + \pi_p \tag{4}$$

Osmotic pressure of brine and permeate are

$$\pi_b = 0.7994\ C_b\ [1 + 0.003(T - 25)] \tag{5}$$

$$\pi_p = 0.7994\ C_p\ [1 + 0.003(T - 25)] \tag{6}$$

Water transport parameter at a specified seawater temperature is corresponding to temperature correction factor and fouling parameter as presented in Eq. (7) (Al-Obaidi et al., 2018).

$$A_{W(T)} = A_{W(25\ C)}\ TCF_p\ F_f \tag{7}$$

Temperature correction factor based on upper and lower of 25 °C

$$TCF_p = exp[0.0343\ (T - 25)]\ ;\ < 25\,^{\circ}C \tag{8}$$

$$TCF_p = exp[0.0307\ (T - 25)]\ ;\ > 25\,^{\circ}C \tag{9}$$

Permeate flow rate is basically the multiplication of water flux and membrane area

$$Q_p = Jw\ A \tag{10}$$

Salinity of brine is the average of both feed and retentate salinities

$$C_b = \frac{C_f + C_r}{2} \tag{11}$$

Solute flux is affected by the solute transport parameter of the membrane and the concentration difference

$$J_s = B_{s(T)}\left(C_w - C_p\right) \tag{12}$$

Solute transport parameter of the membrane is

$$B_{s(T)} = B_{s(25\ C)}\ TCF_p \tag{13}$$

Salinity at the membrane wall

$$C_w = C_p + \left(\frac{C_f + C_r}{2} - C_p\right) exp\left(\frac{Q_p/Q_m}{k}\right) \tag{14}$$

Mass transfer coefficient

$$k = 0.664\ k_{dc}\ Re_b^{0.5}\ Sc^{0.33}\left(\frac{D_b}{d_h}\right)\left(\frac{2d_h}{L_f}\right)^{0.5} \tag{15}$$

Reynolds number and seawater density are

$$\mathrm{Re} = \frac{\rho_b d_h Q_b}{t_f\ w\ \mu b} \tag{16}$$

$$\rho_b = 498.4\ m_f + \sqrt{\left[248400\ m_f^2 + 752.4\ m_f C_b\right]} \tag{17}$$

$$m_f = 1.0069 - 2.757 \times 10^{-4}\ T \tag{18}$$

Schmidt number, viscosity, diffusion coefficient are

$$Sc = \frac{\mu b}{\rho_b D_b} \tag{19}$$

$$\mu_b = 1.234\ \times\ 10^{-6}\ \exp\left\{0.0212\ C_b + \frac{1965}{T + 273.15}\right\} \tag{20}$$

$$D_b = 6.72510^{-6} exp\left\{0.154610^{-3}\ C_b - \frac{2513}{T + 273.15}\right\} \tag{21}$$

Water recovery, solute rejection and specific energy consumption are

$$WR\% = \frac{Q_p}{Q_f} \times 100 = \frac{(C_r - C_f)}{(C_r - C_p)} \times 100 \tag{22}$$

$$SR\% = \frac{C_f - C_p}{C_f} \times 100 \tag{23}$$

$$EC_{pump} = \frac{(P_f\ Q_f \times 101325) \times 36 \times 10^5}{Pump_{eff}\ Qp} \tag{24}$$

Note, Lu et al. (2007) who used spiral wound membrane did not consider temperature and fouling factor dependent water and salt permeability constants. Inclusively, these are considered in Eqs. (7)–(9) and (13). Also, the correlations for the calculation of osmotic pressure and mass transfer co-efficient were quite different. Finally, temperature dependent correlations for the calculations of density, diffusivity and viscosity were not considered. Note, these features are very important for this study as we are subjecting the membrane to a wide range of seawater temperature.

3. Model validation

To quantify the accuracy of the model presented in Section 2, this section utilises the model validation against a set of original data gathered from the RO system of Arab Potash Company (APC) located in Jordan. This is specifically carried out by comparing the gathered data with the model predictions. Table 1 provides the model validation with an average accuracy above 98%. The gPROMS (general Process Modelling System) model builder was used to solve the model equations and carry out the simulation (Process system Enterprise Ltd., 2001).

4. Sensitivity analysis of RO membrane process

A sensitivity analysis of the spiral wound RO membrane process is carried out in this section. This simulation is aimed to find the general effect of varying the operating conditions within selected ranges. In this regard, the simulation of this study was planned to evaluate the responses against the variation of one inlet parameter at a time while other parameters being fixed.

Table 2 presents the full detail of the selected inlet parameters of seawater that will be applied to the RO membrane process. In this regard, the seawater salinity and temperature were selected as same as the ones of the seawater specifications of the Arabian Gulf and specifically Kuwait State (Pokavanich et al., 2013; Ibrahim and Badawy, 2014). However, the feed pressure and flowrate were selected within the

Table 1
The model validation (Adapted from Al-Obaidi et al., 2018).

Parameter	Units	Original data	Model predictions	Error %
Permeate salinity	ppm	1.96	2.03	−3.86
Permeate flow rate	m^3/h	24.57	24.13	1.78
Water recovery	–	83.5	82.01	1.78
Solute rejection	–	95.5	95.501	−1.59

Table 2
Inlet parameters of seawater for the RO membrane process (Base Case).

Inlet parameters	Nomenclature	Set point
Feed salinity	Cf	40 kg/m^3 (40000 ppm)
Feed temperature	*Tf*	32 °C
Feed pressure	*Pf*	60 atm
Feed flowrate	*Qf*	0.03 m^3/s

bounds of the membrane specifications. The characteristics of the membrane selected, and the upper and lower bounds (recommended by the manufacturer) are given in Table 3.

4.1. Effect of seawater salinity

The feed salinity is an important input parameter in the RO process that should be examined against the process performance. This is due to an expected variation of feed salinity due to the existence of different sources of seawater of different salinities.

In this section, the feed salinity was varied between 25 and 45 kg/m^3 (25000 ppm–45000 ppm) including the base case of 40 kg/m^3 (Table 2). The simulation results of solute rejection, water recovery, permeate salinity, retentate salinity, and energy consumption are plotted in Table 4.

Apparently, the obtained results of all the performance indicators show a considerable influence of the feed salinity except the solute rejection. To systematically represent the influence of feed salinity, the variations of process responses are figured out as represented in the next sections.

4.1.1. Effect of seawater salinity on solute rejection and water recovery

The solute rejection has not been considerably changed within the selected feed salinity where it keeps within 99% efficiency. The variation of feed salinity has insignificant influence of less than 0.5% on solute rejection. The insignificant change of solute rejection can be attributed to incomparable increase of permeate salinity against the increase of feed salinity. However, the increase of permeate salinity causes a little reduction of solute rejection due to increasing the solute flux with increasing feed salinity. On the other hand, the water recovery has noticed a considerable variation throughout the selected change of salinity. The maximum water recovery was obtained at the lowest applied salinity. This is attributed to a lower osmotic pressure that can be obtained at the lowest feed salinity. Increasing the osmotic pressure is simply causing a decrease in the driving force of water flux that leading to a decreased on the overall water recovery (Sassi and Mujtaba, 2012). Therefore, it is plausible to confirm the highest permeated water at the lowest salinity through the membrane pores that satisfies the maximum water recovery. Fig. 2 shows the behaviors of solute rejection and water recovery against the considered variation of feed salinity. Statistically, the water recovery decrease by 54% as a response to an increase in the feed salinity from 25 to 45 kg/m^3, which can be considered as a remarkable influence for RO membrane system.

Table 3
Membrane characteristics and allowed limits of operation.

Parameter	Value	Unit
Membrane	SW30HRLE-400i	–
Supplier	DOW FILMTECK	–
Membrane material and module configuration	Polyamide thin-film composite Spiral wound element	–
Maximum operating pressure	83	atm
Maximum operating feed flow rate	0.00536	m^3/s
Minimum operating feed flow rate	0.001	m^3/s
Maximum pressure drop per element	0.987	atm
Maximum operating temperature	45	°C
Module length (L)	1	m
$A_{w(T_o)}$ (m/atm s) at 25 °C	9.509656x10^{-7}	m/s atm
$B_{s(T_o)}$ NaCl (m/s) at 25 °C	5.64589x10^{-8}	m/s
Spacer type	Naltex-129	–
Feed spacer thickness (t_f)	0.000593	m
Length of spacer in the spacer mesh	2.77x10^{-3}	m
Feed spacer characteristic (A')	7.38	–
Feed spacer characteristic (n)	0.34	–
Voidage (ε)	0.9058	–

Table 4
Effect of seawater salinity on the performance metrics.

Cf (kg/m^3)	*SR%* (–)	*WR%* (–)	C_P (ppm)	C_r (kg/m^3)	*EC* (kWh/m^3)
25	99.748	34.259	62.9	37.995	5.799
30	99.718	29.873	84.3	42.744	6.650
35	99.682	25.832	111.1	47.151	7.690
40 (Base case)	99.637	22.075	145.2	51.290	8.999
45	99.577	18.560	190.1	55.212	10.704

4.1.2. Effect of seawater salinity on permeate and retentate salinities

Based on the simulation results described in the above section, it is not complicated to predict the behaviors of permeate salinity and retentate salinity against the variation of feed salinity. Table 4 and Fig. 3 present the simulation results. In this regard, the increase of feed salinity causes an increase in the permeate salinity and retentate salinity. The increase of permeate salinity is attributed to an increase in solute flux. However, increasing of feed salinity would definitely increase the retentate salinity since RO membrane process is basically a water filtration approach where any increase of feed salinity would increase the bulk salinity and the discharged one. Statistically, increasing the feed salinity from 25 to 45 kg/m^3 causes an increase of 67% in permeate salinity and 45% in retentate salinity.

4.1.3. Effect of seawater salinity on energy consumption

One of the most critical factors in any industrial process is the energy consumption that need to be minimised as much as possible. Occasionally, RO process characteristics by its low energy consumption compared to the other thermal desalination technologies. Table 4 and Fig. 4 depict a direct relationship between feed salinity and consumed energy. More specifically, an increase in feed salinity causes an increase in the specific energy consumption. The explanation of this behaviour is that increasing the feed concentration causes a reduction of water flux and total permeate flowrate that correspondingly related to water recovery and energy consumption. Statistically, increasing the feed

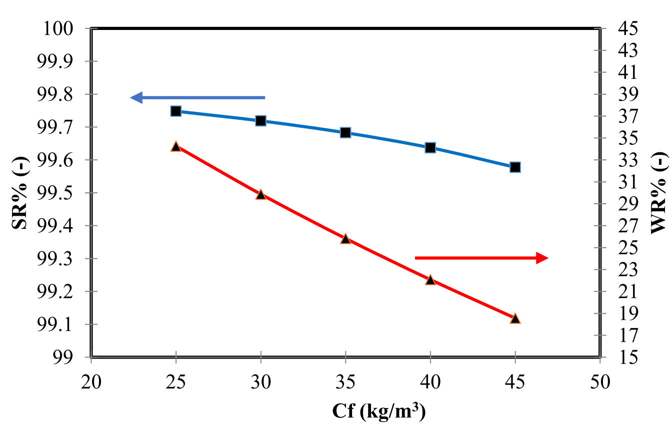

Fig. 2. Effect of seawater salinity on solute rejection and water recovery.

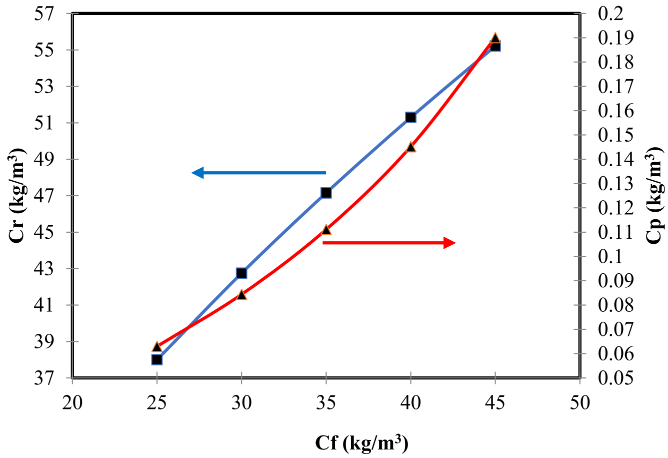

Fig. 3. Effect of feed salinity on retentate and permeate salinities.

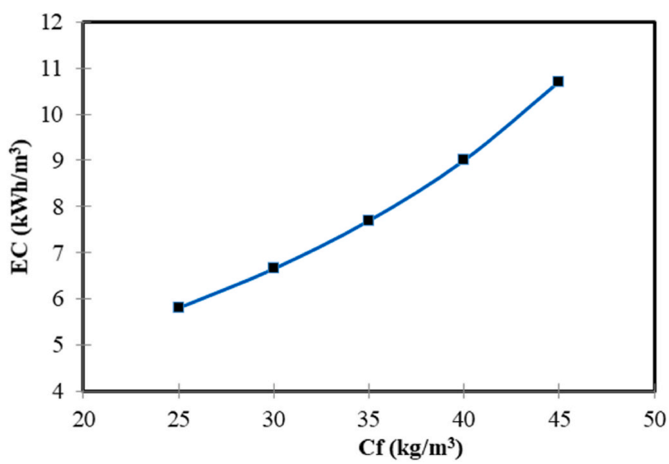

Fig. 4. Effect of feed salinity on specific energy consumption.

concentration from 25 to 45 kg/m^3 leads an increase of 84.4% in specific energy consumption. Thus, it is affordable to apply low feed salinity to ensure low energy consumption besides high water recovery.

4.2. Effect of feed pressure

The feed pressure is related to the design operation of a selected process that drives using a cylindrical pump. In this regard, it is fair to expect a failure of pump or damage of the membrane that would probably lead to an increase or decrease in the supplied pressure. Therefore, it would be advantageous to carry out simulation-based model developed to explore the influence of feed pressure on the process efficiency.

In this section, a variation of feed pressure between 60 and 80 atm was applied and the simulation results of several performance indicators of the RO membrane were obtained and listed in Table 5. The variation of feed pressure is considered at constant feed flowrate, salinity, and temperature as listed in Table 2.

Table 5
Effect of operating pressure.

Pf (atm)	*SR%* (−)	*WR%* (−)	C_P (ppm)	C_r (kg/m^3)	*EC* (kWh/m^3)
60 (base case)	99.637	22.075	145.2	51.290	8.999
65	99.678	25.556	128.4	53.687	8.421
70	99.709	28.904	116.2	56.215	8.019
75	99.732	32.118	107.1	58.875	7.732
80	99.750	35.193	99.8	61.668	7.527

4.2.1. Effect of feed pressure on solute rejection and water recovery

Table 5 and Fig. 5 represent that increasing of feed pressure has a considerable influence on the water recovery. Specifically, Fig. 5 shows that an increase in feed pressure from 60 to 80 atm obtains a rise of 37.5% in water recover from 22% to 35.2%. However, increasing feed pressure has a slight growth in solute rejection of less than 1% from 99.63% to 99.75%. The reason behind this behavior is that increasing the feed pressure would increase the water flux, which can boost the permeate flowrate and enhance water recovery. The obtained results are in agreement with the findings of Al-Obaidi and Mujtaba (2016). However, the marginal improvement of membrane rejection is attributed to an increase in the rate of dilution in the permeate channel due to increasing the water flux through the membrane pores.

4.2.2. Effect of feed pressure on permeate and retentate salinities

Increasing operating pressure results in an increase in water flux as described above and therefore it is fair to expect a reduction of permeate salinity in the permeate channel. Table 5 and Fig. 6 show that increasing the operating pressure has decreased the permeate salinity with accommodating an increase of retentate salinity. Basically, these results are cooperated with the ones resulted for solute rejection and water recovery (Fig. 5). Statistically, increasing feed pressure from 60 to 80 atm is enough to decrease the permeate salinity by 68.7% and increase the retentate salinity by 20%. Therefore, feed pressure must be carefully controlled to prevent the impairment of product quality and secure low salinity of product (Abbas, 2005).

4.2.3. Effect of feed pressure on the specific energy consumption

The influence of increasing the feed pressure on specific energy consumption is depicted in Table 5 and Fig. 7. In this regard, increasing of feed pressure causes a decrease in the specific energy consumption due to producing high permeate flowrate at high pressures compared to low pressures despite the expense of more energy to run the pump at high pressures. These results are also confirmed by Sassi and Mujtaba (2011). Statistically, increasing feed pressure from 60 to 80 atm causes a remarkable decrease of energy consumption by 16.4%.

4.3. Effect of seawater temperature

The variation of temperature throughout the year is expected due to the variation of seasons. Therefore, it is acceptable to explore the process performance against the variation of temperature. In this section, a variation of feed temperature is tested between 22 °C and 35 °C on the performance indicators of the RO membrane process besides attaining fixed values of feed pressure, salinity, and flow rate as represented in

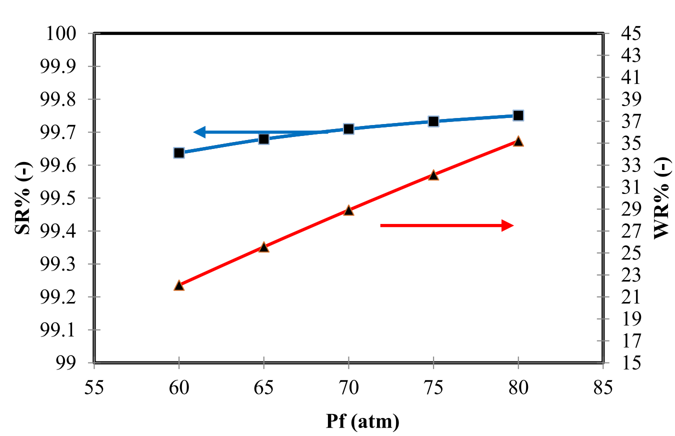

Fig. 5. Effect of feed pressure on solute rejection and water recovery.

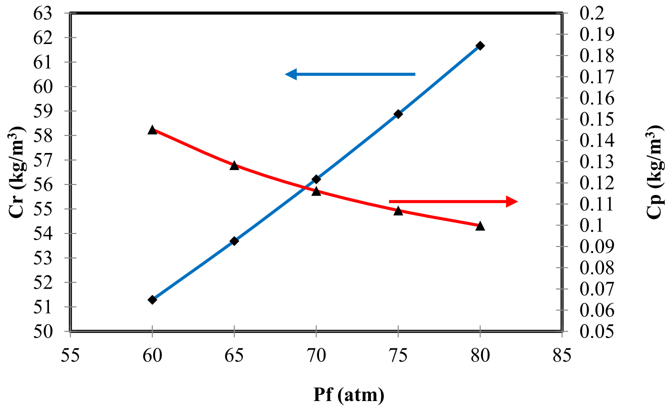

Fig. 6. Effect of feed pressure on retentate and permeate salinities.

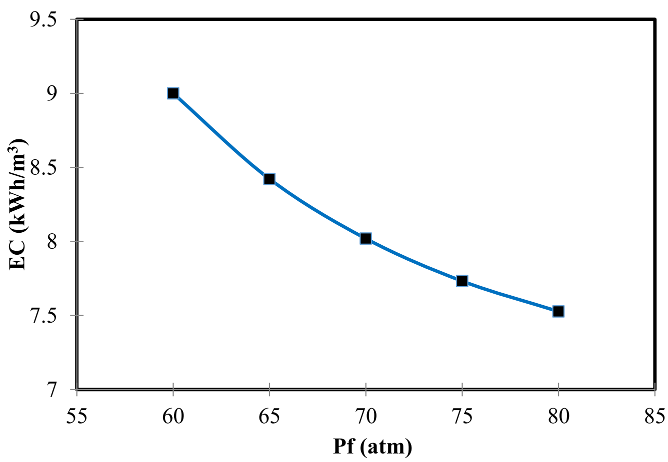

Fig. 7. Effect of feed pressure on specific energy consumption.

Table 2. The overall simulation results are given in Table 6. The obtained results confirm insignificant influence of feed temperature on the responses of the RO membrane system. These results are discussed in detail in detailed figures as will be represented in the upcoming sections.

4.3.1. Effect of feed temperature on the solute rejection and water recovery

Fig. 8 shows the changes of solute rejection and water recovery as a result to an increase in the feed temperature from 22 °C to 35 °C. A growth of feed temperature causes a maximum increase of 10% in water recovery. This is attributed to a decrease in the viscosity and density properties as a consequence to increasing the feed temperature. Therefore, an enhancement of water permeation through the membrane pores is expected with increasing the supplied temperature. These results are commensurate with the findings of Al-Mutaz and Al-Ghunaimi, 2001 and Sassi and Mujtaba (2012). Occasionally, the simulation results of increasing feed temperature show a slight increase of solute rejection of around 0.03%. The slight improvement of solute rejection is mainly

Table 6
Effect of operating temperature.

Tf (°C)	*SR%* (−)	*WR%* (−)	C_p (ppm)	*Cr* (kg/m^3)	*EC* (kWh/m^3)
22	99.610	21.122	155	50.669	9.406
25	99.619	21.429	152	50.868	9.271
27	99.624	21.623	150	50.994	9.187
32 (base case)	99.637	22.075	145	51.290	8.999
35	99.643	22.323	142	51.454	8.899

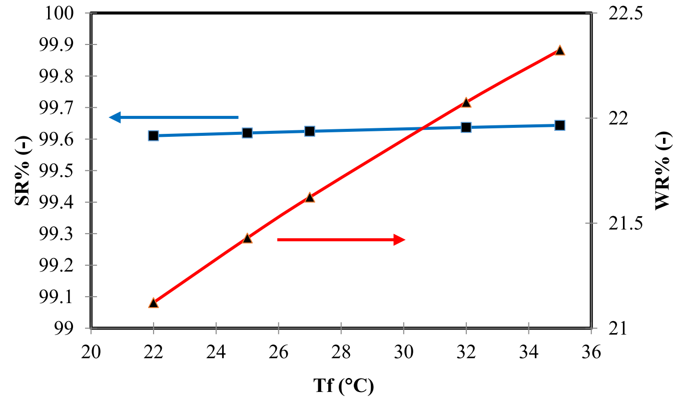

Fig. 8. Effect of feed temperature on solute rejection and water recovery.

attributed to an improvement of permeate salinity that will be discussed in the next section.

4.3.2. Effect of feed temperature on the permeate and retentate salinities

Fig. 9 elucidates that an increase of feed temperature has insignificant influence on both the permeate salinity and retentate salinity. As mentioned earlier, increasing the feed temperature from 22 °C to 35 °C would increase the water transport parameter that means an increase in the water flux. This in turn causes a decrease in permeate salinity at the permeate channel that corresponding to an increase in retentate salinity. Statistically, the considered increase of temperature causes a drop of permeate salinity by 8.5% and 1.5% increase of retentate salinity.

4.3.3. Effect of feed temperature on the specific energy consumption

Fig. 10 assesses the relation between the feed temperature and specific energy consumption. This is basically presenting a reduction of specific energy consumption due to increasing the supplied temperature. Fig. 10 indicates a considerable drop of specific energy consumption for an increase of 10 °C. This might be attributed to the improvement of water flux through the membrane pores due to increasing temperature of the bulk fluid. This is also accompanying an increase of pore's size with high mobility of water due to reduced viscosity and density. Statistically, Fig. 10 affirmed a drop of specific energy consumption by 4.5% due to raise temperature from 22 °C to 35 °C. The same trend of these results was confirmed by Al-Mutaz and Al-Ghunaimi, 2001. Therefore, it would be affordable to operate the RO process at elevated temperatures without exceeding the limited constrain of the membrane's manufacturer given in Table 3.

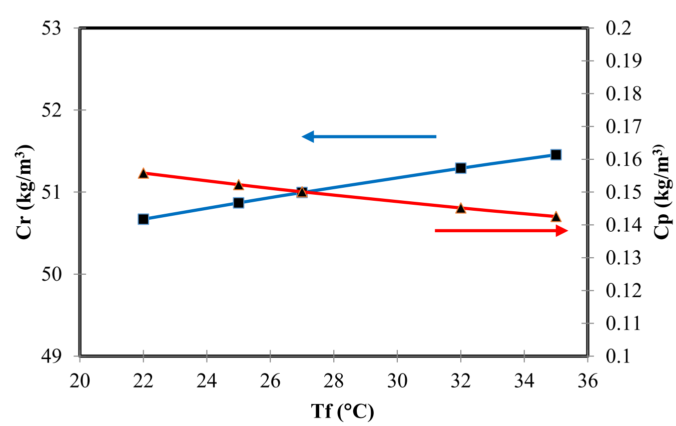

Fig. 9. Effect of feed temperature on retentate and permeate salinities.

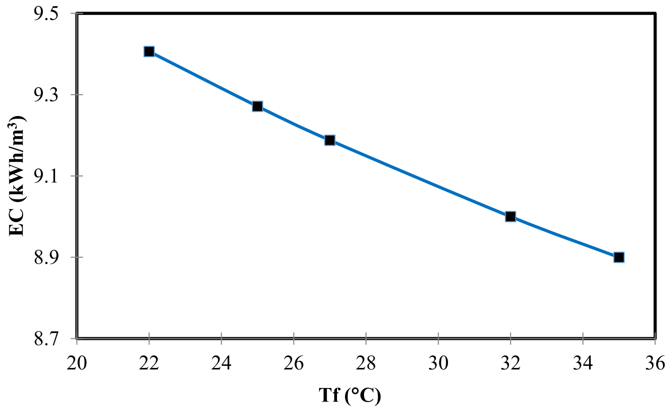

Fig. 10. Effect of feed temperature on specific energy consumption.

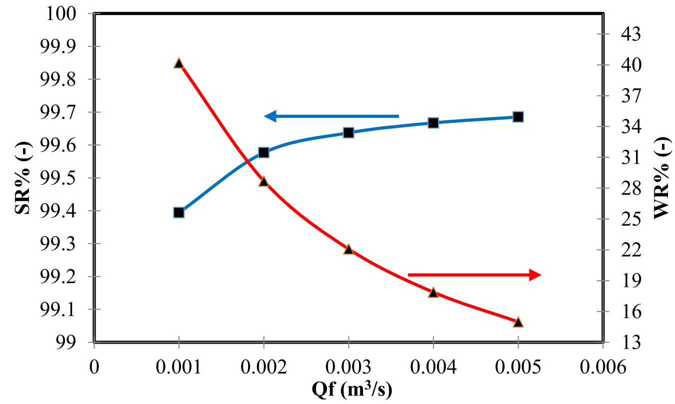

Fig. 11. Effect of feed flowrate on solute rejection and water recovery.

4.4. Effect of seawater feed flowrate

Feed flowrate of RO process is originally designed based on the membrane's recommendation that specifies the upper and lower limits with warning to be exceeded. It is vital to study the influence of feed flowrate (within the acceptable range) to quantify the unexpected conditions of pump failure or to explore the feasible value that gain the highest efficiency. Therefore, this section exhibits a variation of feed flowrate from 0.001 m^3/s to 0.005 m^3/s and recording the responses of solute rejection, water recovery, permeate salinity, retentate salinity, and specific energy consumption. An overview of the simulation results of Table 7 indicates a noticeable influence of feed flowrate on the performance indicators. However, this simulation has already considered fixed feed salinity, pressure, and temperature as reported in Table 2.

4.4.1. Effect of feed flowrate on solute rejection and water recovery

Fig. 11 shows that an increase in feed flowrate causes a slight increase in solute rejection that can be ascribed to increasing of rate of turbulent inside the feed channel. This is basically related to an increase in the mass transfer coefficient and correspondingly increases the water flux. Therefore, this influence would diminish the permeate salinity and enhance the solute rejection. Statistically, the variation of feed flowrate induces an increase of 0.029% in solute rejection. On the other hand, Fig. 11 demonstrates a significant impact of increasing feed flowrate on the water recovery where it decreases by around 62%. Again, increasing the feed flowrate is simply means a lower residence time of the fluid inside the membrane module that would significantly reduce the filtration time and cause a reduction of water flux.

4.4.2. Effect of feed flowrate on the permeate and retentate salinities

The effects of increasing feed flowrate on the permeate and retentate salinities are represented in Fig. 12. This is specifically elucidated an exponentially decrease in both permeate and retentate salinities. Increasing the feed flowrate would trigger the mass transfer coefficient due to a high agitation rate at high velocities that encountered with reduced the solute salinity on the membrane wall and reducing the solute flux via membrane's pores. Moreover, increasing the rate of turbulence due to increasing feed velocity will reduce the retentate salinity as depicted in Fig. 12. Statistically, increasing the feed flow rate from 0.001 to 0.005 m^3/s has associated with a decrease of permeate salinity by 48% and retentate salinity by 29.5%. These are fantastic results to be applied for RO membrane process that justified a simultaneous reduction of both permeate and retentate salinities.

Table 7
Effect of operating flowrate.

Qf (m^3/s)	*SR%* (−)	*WR%* (−)	C_P (ppm)	C_r (kg/m^3)	*EC* (kWh/m^3)
0.001	99.394	40.198	242.2	66.724	4.942
0.002	99.576	28.694	169.3	56.028	6.923
0.003	99.637	22.075	145.2	51.290	8.999
0.004	99.667	17.870	133.1	48.674	11.117
0.005	99.685	14.982	125.9	47.026	13.260

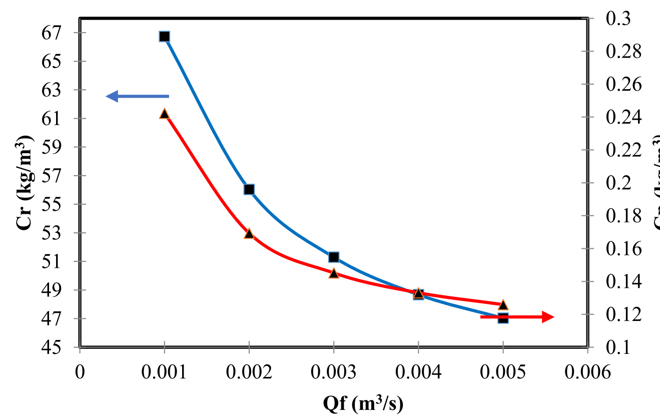

Fig. 12. Effect of feed flowrate on retentate and permeate salinities.

4.4.3. Effect of feed flowrate on the specific energy consumption

The investigation of increasing the feed flowrate on energy consumption is depicted in Fig. 13 at fixed other inlet parameters of RO process. This in turn confirmed an increase in the specific energy consumption as a response to increased flowrate. The reason behind this behavior is that the pressure drop increases due to an increase in the rate of corrosion with increasing the feed flow rate. This would reduce the

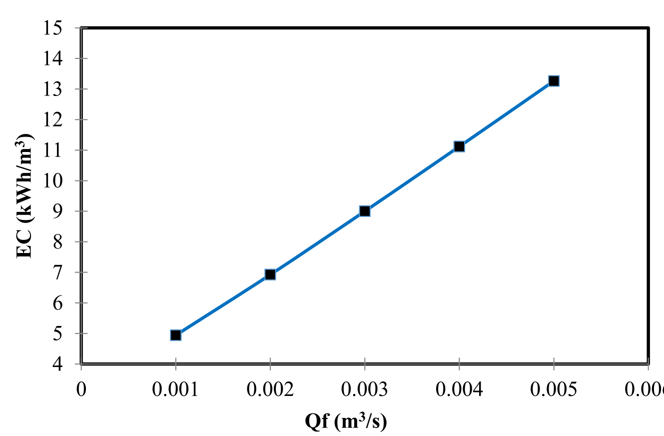

Fig. 13. Effect of feed flow rate on specific energy consumption.

motivation of water flux (pressure difference). Therefore, permeate flowrate will be decreased that means an increase of specific energy consumption. Statistically, increasing the feed flow rate from 0.001 m^3/s to 0.005 m^3/s causes an increase of specific energy consumption by 62.7%.

4.5. Critical review of simulation results of the RO membrane system

The RO simulation-based modelling process helps to explain the role of all control variables that influence process efficiency without the need for long, costly, and complex experimentations (Li et al., 2017). The assembly of the appropriate RO process indicators, such as saline desalination ratio, energy use and solvent rejection, can therefore be illustrated by modelling the flow rate control variables, pressure, temperature, and design variables of the membrane unit dimension (Siddique et al., 2017). In addition, process variables can be customised by optimisation without any change to the actual plant.

The simulation results indicated that the feed pressure must be carefully increased to improve the product quality with a higher energy saving. However, this simulation has considered increasing pressure at fixed feed flowrate. Therefore, these results are conditioned. Furthermore, increasing the feed temperature can be a costly option, which can be an unnecessary step if minimising energy consumption is the objective function.

The energy consumption considered as one of the important factors in any desalination plant. Given that freshwater is an indispensable commodity, and its production bears the nature of sustainability, reducing the cost of production will contribute to enhancing the continuity of production to provide fresh water to the largest number of people. Furthermore, reducing energy consumption necessarily means reducing gas flaring processes, which reduces harmful emissions such as CO_2 to the environment, which contributes to preserving the environment from the Greenhouse gases. Another important factor that must be monitored is the discharge salinity, where the continuously discharged over the years has a harmful effect on marine life because of increasing the salinity average. This poses a challenge for engineers working on designing desalination plants.

5. Conclusions

Detailed evaluation of the performance (in terms of salt rejection, water quality, water recovery, and specific energy consumption) of a spiral wound membrane using a comprehensive and a realistic model has been presented in this paper. In this regard, a wide range of seawater conditions of salinity and temperature and varying feed pressure and flow rate of RO process were considered in this work. The results indicated that increasing two parameters, the feed pressure and temperature, can positively improve the RO membrane performance in terms of productivity and specific energy consumption. Increasing feed temperature enhances the water flux and reduces the permeate salinity resulting in reduction in specific energy consumption. On the contrary, increasing the feed salinity and flowrate have a negative influence on the process responses. Note, increasing feed salinity or flowrate leads to increased specific energy consumption and reduced process water recovery.

Declaration of competing interest

There is no conflict of interests.

References

Abbas, A., 2005. Simulation and analysis of an industrial water desalination plant. Chem. Eng. Process: Process Intensification 44 (9), 999–1004.

Al-Mutaz, I.S., Al-Ghunaimi, M.A., 2001. October. Performance of reverse osmosis units at high temperatures. In: The IDA World Congress on Desalination and Water Reuse, pp. 26–31. Bahrain.

Al-Obaidi, M.A., Mujtaba, I.M., 2016. Steady state and dynamic modeling of spiral wound wastewater reverse osmosis process. Comput. Chem. Eng. 90, 278–299.

Al-Obaidi, M., Alsarayreh, A., Al-Hroub, A., Alsadaie, S., Mujtaba, I.M., 2018. Performance analysis of a medium-sized industrial reverse osmosis brackish water desalination plant. Desalination 443, 272–284.

Alsarayreh, A.A., Al-Obaidi, M.A., Patel, R., Mujtaba, I.M., 2020. Scope and limitations of modelling, simulation, and optimisation of a spiral wound reverse osmosis process-based water desalination. Processes 8 (5), 573.

Carter, N.T., 2015. Desalination and membrane technologies: federal research and adoption issues. Congr. Res. Serv. Available at: https://fas.org/sgp/crs/misc/R40477.pdf.

Donguy, J.R., Meyers, G., 1996. Seasonal variations of sea-surface salinity and temperature in the tropical Indian Ocean. Deep Sea Res. Oceanogr. Res. Pap. 43 (2), 117–138.

Du, Y., Xie, L., Wang, Y., Xu, Y., Wang, S., 2012. Optimization of reverse osmosis networks with spiral-wound modules. Ind. Eng. Chem. Res. 51, 11764–11777.

Ibrahim, M., Badawy, R., 2014. A parametric study of the impact of the cooling water site specific conditions on the efficiency of a pressurized water reactor nuclear power plant. Int. J. Nucl. Energy 1–6.

Li, M., 2012. Optimal plant operation of brackish water reverse osmosis (BWRO) desalination. Desalination 293, 61–68.

Li, Y., Xu, Z., Liu, S., Zhang, J., Yang, X., 2017. Molecular simulation of reverse osmosis for heavy metal ions using functionalized nanoporous graphenes. Comput. Mater. Sci. 139, 65–74.

Lu, Y.Y., Hu, Y.D., Xu, D.M., Wu, L.Y., 2006. Optimum design of reverse osmosis seawater desalination system considering membrane cleaning and replacing. J. Membr. Sci. 282, 7–13.

Lu, Y.Y., Hu, Y.D., Zhang, X.L., Wu, L.Y., Liu, Q.Z., 2007. Optimum design of reverse osmosis system under different feed concentration and product specification. J. Membr. Sci. 287, 219–229.

Oki, T., Kanae, S., 2006. Global hydrological cycles and world water resources. Science 313, 1068–1072.

Pokavanich, T., Polikarpov, I., Lennox, A., Al-Hulail, F., Al-Said, T., Al-Enezi, E., Al-Yamani, F., Stokozov, N., Shuhaibar, B., 2013. Comprehensive investigation of summer hydrodynamic and water quality characteristics of desertic shallow water body: Kuwait Bay. J. Coast. Dynam. 12 (2), 1253–1264.

Process System Enterprise Ltd, 2001. gPROMS Introductory User Guide. Process System Enterprise Ltd, London.

Ruiz-García, A., Nuez, I., Carrascosa-Chisvert, M.D., Santana, J.J., 2020. Simulations of BWRO systems under different feedwater characteristics. Analysis of operation windows and optimal operating points. Desalination 491, 114582.

Ruiz-García, A., Nuez, I., 2020. On-off control strategy in a BWRO system under variable power and feedwater concentration conditions. Appl. Sci. 10 (14), 4748.

Saif, Y., Elkamel, A., Pritzker, M., 2008. Global optimization of reverse osmosis network for wastewater treatment and minimization. Ind. Eng. Chem. Res. 47, 3060–3070.

Sassi, K.M., Mujtaba, I.M., 2011. Optimal design and operation of reverse osmosis desalination process with membrane fouling. Chem. Eng. J. 171 (2), 582–593.

Sassi, K.M., Mujtaba, I.M., 2012. Effective design of reverse osmosis based desalination process considering wide range of salinity and seawater temperature. Desalination 306, 8–16.

See, H.J., Vassiliadis, V.S., Wilson, D.I., 1999. Optimisation of membrane regeneration scheduling in reverse osmosis networks for seawater desalination. Desalination 125, 37–54.

Siddique, K., Rizwan, M., Shahid, M.J., Ali, S., Ahmad, R., Rizvi, H., 2017. Textile wastewater treatment options: a critical review. In: Enhancing Cleanup of Environmental Pollutants. Springer.

Villafafila, A., Mujtaba, I.M., 2003. Fresh water by reverse osmosis based desalination: simulation and optimisation. Desalination 155, 1–13.

Wenten, I.G., 2016. Reverse osmosis applications: prospect and challenges. Desalination 391, 112–125.

Woo, Y.C., Kim, S.-H., Shon, H.K., Tijing, L.D., 2019. Introduction: membrane desalination today, past, and future. In: Basile, A., Curcio, E., Inamuddin (Eds.), Current Trends and Future Developments on (Bio-) Membranes. Elsevier (xxv-xlvi).